Journal of Crystal Growth 629 (2024) 127580

Contents lists available at ScienceDirect

Journal of Crystal Growth

journal homepage: www.elsevier.com/locate/jcrysgro

# Bismuth chalcogenide topological insulators crystals grown by the optical floating zone technique

A. Guarino [a,*], R. Arumugam [a], R. Fittipaldi [a,*], M. Lettieri [a], G. Balakrishnan [b], A. Vecchione [a]

[a] CNR-SPIN, c/o Università di Salerno, Via Giovanni Paolo II, 132, 84084, Fisciano (SA), Italy
[b] Department of Physics, University of Warwick, Coventry CV4 7AL, United Kingdom

ARTICLE INFO

*Keywords:*
Bismuth compounds
Floating zone technique
Single crystal growth
X-ray diffraction
Characterization

ABSTRACT

In this paper, two procedures for the growth of both binary and ternary single crystals of bismuth chalcogenides by optical floating zone technique are described. Detailed characterization has been carried out on a series of samples, i.e. $Bi_2Se_xTe_{3-x}$, with x = 0 and 0.9, and $Bi_{2-x}Sb_xSe_3$, with x = 0 and 0.15, to isolate high quality single crystals, essential for an accurate study of the physical properties of the materials. Systematic compositional and structural analysis on the samples grown by the two different procedures have been compared to infer the optimal growth parameters to obtain the largest possible single crystals. The *c*-axis lattice parameter of $Bi_{1.85}Sb_{0.15}Se_3$ is reported here for the first time.

## 1. Introduction

Bismuth telluride and bismuth selenides are functional thermoelectric materials for low- and near-room temperature applications because of their low thermal conductivity and high weighted mobility [1]. In the last decade, a large effort has been devoted to the study of this family of materials due to their excellent topological properties [2,3]. The development of a growth method to obtain pure materials with on-demand band gap is of utmost importance to investigate the equilibrium and out-of-equilibrium properties of low bandgap and metallic samples. High quality single crystals are essential for determining the intrinsic properties of topological insulators avoiding the influence of grain boundaries and impurity phases as is the case in their polycrystalline counterparts [4]. Topological materials like metal chalcogenides are available as single crystals grown by several techniques such as Bridgman [5,6], Czochralski [7], and self-flux [8,9]. Several different physical and chemical methods have been utilized to study thin films [10–12]. Some reports of the growth of chalcogenides by floating zone (FZ) technique have been recently published [13–15]. This technique has the advantage of having a steep temperature gradient to melt a small portion of a polycrystalline feed rod which is encapsulated in an ampoule. The molten region will push impurities to one end of the feed rod and as it moves through the ampoule during the growth, giving purer solidified material. Typically, chalcogenides such as bismuth telluride or selenide grown using the FZ method have a better crystalline uniformity than ones grown using the traditional vertical Bridgman or Czochralski techniques. Moreover, the congruent melting property of bismuth telluride and selenide makes the growth of single crystals from the melt easier. Consequently, the sizes of the crystals grown by the FZ technique are much larger than those that can be obtained by the flux technique. Since for many studies large and defect free crystals are desirable, the FZ technique is the ideal route to produce such samples. In the case of bismuth chalcogenides, to avoid oxidation of the materials, the stoichiometric mixture is placed in a sealed quartz tube and the melt process is carried out in the same tube. Therefore, the first steps in the preparation of the materials are crucial to guarantee the high quality of the crystals.

The doping of $Bi_2X_xTe_{3-x}$ (X = Se or Sb) in the whole 'x' range results in small variations of the lattice parameters of the crystalline cell but does not affect the space group which remains the same as the parent compound [10,16]. Hence, even the crystals of doped compounds can be easily exfoliated thanks to the "quintuple layers" that are repeated in the structure and are linked together by weak van der Waals forces. On the other hand, the physical properties change with doping: as an example, the band gap of the samples increases for certain doping values of Se and Sb in $Bi_2Te_3$ [17,18]. Although the properties of the Bi-Se-Sb system are not well studied and reported, there is a slight increase of the optical band gap by increasing the antimony concentration from x = 0 to x = 0.2 in $Bi_{2-x}Sb_xSe_3$ films [19].

In this work, high quality single crystals of pure $Bi_2Se_3$ and $Bi_2Te_3$ as

* Corresponding authors.
*E-mail addresses:* anita.guarino@spin.cnr.it (A. Guarino), rosalba.fittipaldi@spin.cnr.it (R. Fittipaldi).

https://doi.org/10.1016/j.jcrysgro.2024.127580
Received 24 October 2023; Received in revised form 3 January 2024; Accepted 8 January 2024
Available online 10 January 2024

well as crystals with concentrations of Sb and/or Se corresponding to the maximum possible values of the band gap reported in the literature were grown by using optical floating zone technique. Morphology, composition and crystalline structure were described for the various single crystals, synthesized using two different growth procedures.

## 2. Experimental

The optimised procedure for growing single crystals of the Bi-based samples requires a period of two weeks. The high purity starting elements (Bi, 99.997 %, Alfa Aeser; Se, 99.999 %, Alfa Aeser; Te, 99.999 %, Aldrich; Sb, 99.5 %, Sigma Aldrich) weighed in stoichiometric ratios were placed in a quartz tube and sealed in a vacuum of $10^{-5}$ mbar. Two different procedures were followed to grow the material, one in one step (Procedure I), the other in three steps (Procedure II), as shown in the Table 1. In both procedures, the sealed quartz tube was placed in an alumina crucible in vertical position inside a muffle furnace during the thermal treatments. Procedure I consisted of a single treatment, the same for all compounds, heating up to a temperature of 820 °C (100 °C/h), then cooling down slowly to 540 °C (3 °C/h) and finally quenching the material from 540 °C to room temperature. The Procedure II consisted of different dwell temperatures adopted for each step depending on the compounds (see Table 1). During the first steps of Procedure II, we begin by heating the starting elements at a temperature close to the melting point of each compound. This enables mixing and ensures that the final phase is homogeneous. $Bi_2Te_3$ and related compounds have a melting point of approximately 600 °C, while $Bi_2Se_3$ and related compounds melt at around 700° [20]. To ensure complete melting of the materials, we set the temperature of the mixture to be at least 50 °C higher than their respective melting points. Additionally, the sealed quartz tube was taken out of the furnace and turned upside down between each of the heat treatment steps, in an attemp to further improve the mixing of the elements and ensuring phase homogeneity. At the end of each thermal treatment, the samples were quenched to room temperature. We do not need to set slow cooling among the three thermal steps, saving time for the following growth process. Indeed, after this first heating cycle, for both the Procedures used, the quartz tubes were found to already contain highly crystalline materials of the compounds.

In a further cycle of heat treatment in the optical floating zone furnace (NEC Machinery, model SC1-MDH11020), the material was melted again within a high thermal gradient using a very low translation speed, favoring the solidification of larger crystals. To perform floating zone (FZ) growth, the quartz tubes produced from the heating using Procedures I and II were directly suspended in the image furnace, in the place of the conventional feed rod. The power of the lamps required to melt the material in the quartz tubes varied between 90 and 130 W. For all the growths, rotation and translation feed velocity were fixed at 20 rpm and 0.5 mm/h, respectively. In accordance with the temperature phase diagrams of Bi-Se and Bi-Te systems [20], higher values of the lamps power were required to melt $Bi_2Se_3$ and $Bi_{2-x}Sb_xSe_3$ samples.

All the grown samples were systematically characterized to investigate the morphology and stoichiometry by using scanning electron microscopy (SEM-LEO, Model EVO 50) and energy dispersive spectroscopy (EDS), respectively. Several crystals were selected by cleaving the as-grown boule. In our optimized conditions, the boule can be cleaved along the growth axis, which happens to be perpendicular to the *c*-axis of the crystals. In addition, x-ray diffraction measurements were performed to investigate the crystalline quality of the samples by using a Bruker D2 PHASER 2nd generation with CuKα radiation of 1.54 Å. Electron backscattered diffraction was carried out using a Inca Crystal 300 detector, added to the SEM with a LaB6 gun.

## 3. Results and discussion

### 3.1. Morphology and composition

A comparison of the size and morphologies of $Bi_2Te_3$ crystals grown with the two different Procedures is reported in Fig. 1. Each panel of the Fig. 1 contains a picture of the sample and a SEM image with details of its morphology. An example of small crystals formed just after the Procedure II is shown in Fig. 1a), while, in Fig.s 1b) and 1c) are presented crystals obtained after the FZ growth using the quartz tubes treated with Procedure I and II, respectively. It is worth noting that the FZ growth clearly increases the size of the crystals, and the use of Procedure II improves the homogeneity of the samples. This aspect is highlighted by the SEM analysis of the crystals. The image in Fig. 1a) shows the typical morphology of the crystals grown in the muffle furnace. EDS analyses performed on that samples confirm that they have the correct stoichiometry, while from electron backscattered diffraction (EBSD) measurements, it has been inferred that they are most likely still polycrystalline, as will be described in subsection 3.2. In Fig. 1b) is shown the morphology observed on average for crystals synthesized by Procedure I and then processed by the FZ method in the image furnace.

The surface appears rough containing many particles with different shapes. EDS analyses performed on this kind of samples point to the presence of some oxygen and silicon contaminations, likely due to the reactions of the powder materials with the quartz tube walls. Finally, Fig. 1c) is an example of flat cleaved-surface typically observed for crystals obtained by the synthesis with the Procedure II followed by the FZ growth.

Fig. 2 and Fig. 3 show the EDS elements maps of two crystals grown by Procedure I + FZ and Procedure II + FZ, respectively. Both the figures show the SEM image of the investigated area and the maps of Bi and Te. In the case of the crystal in Fig. 2, some small clusters of Te as well as particles of silicon oxide likely coming from the quartz tube walls (see bottom panels of the figure) are observed, while in the maps of Fig. 3 the elements distribution is homogeneous in the whole investigated area. Although both Procedure I and Procedure II entail melting the material, the rotation step described in Procedure II favors the mixing of the materials to homogenize the melt. Additionally, it's worth noting that, in the case of $Bi_2Te_3$ samples, the maximum temperature reached in Procedure I is 820 °C, while it is only 690 °C in Procedure II. As a result, Procedure I is seen to cause a reaction of the materials with the walls of the quartz tube due to the higher temperature used. Similar investigations have been performed on the different compounds with similar results. In particular, EDS analyses confirm the correct

**Table 1**
Thermal treatments performed on the sealed quartz tube to grow the materials, following the two optimized Procedures.

| | Procedure I | Procedure II | | |
|---|---|---|---|---|
| $Bi_2Te_3$, $Bi_2Se_xTe_3$ | 100°C/h, 820°C/h, 24 h, 3°C/h, 540°C/h, 24 h | 250°C/h, 650°C/h, 12 h | 250°C/h, 650°C/h, 12 h | 250°C/h, 690°C/h, 24 h, 7°C/h, 550°C/h, 15 h |
| $Bi_2Se_3$, $Bi_{2-x}Sb_xSe_3$ | | 250°C/h, 750°C/h, 12 h | 250°C/h, 750°C/h, 12 h | 250°C/h, 820°C/h, 24 h, 10°C/h, 540°C/h, 15 h |

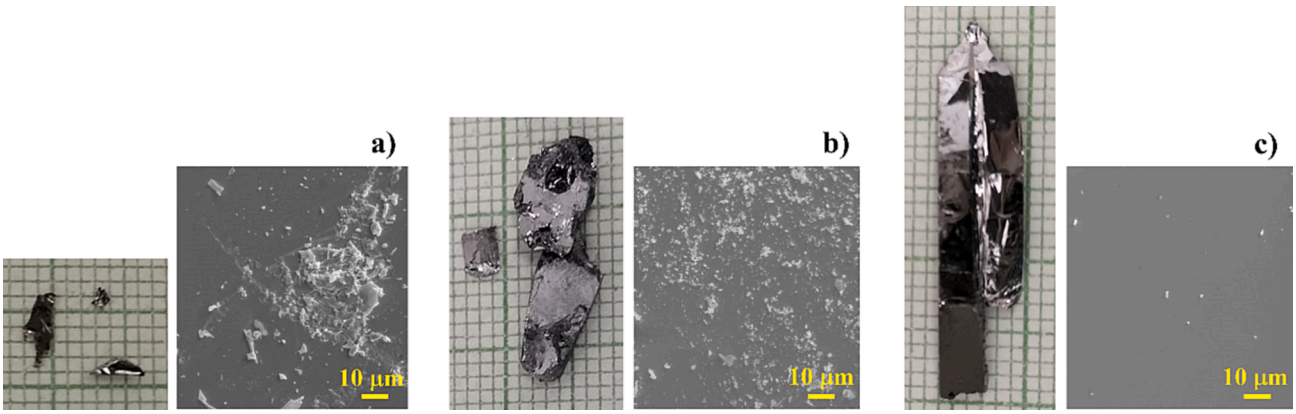


**Fig. 1.** Examples of $Bi_2Te_3$ single crystals after a) the Procedure II, b) the Procedure I + FZ, c) the Procedure II + FZ. Each panel contains a picture of the sample and a SEM image with details of its morphology. The crystals were imaged on graph paper, with each square representing 1 $mm^2$.

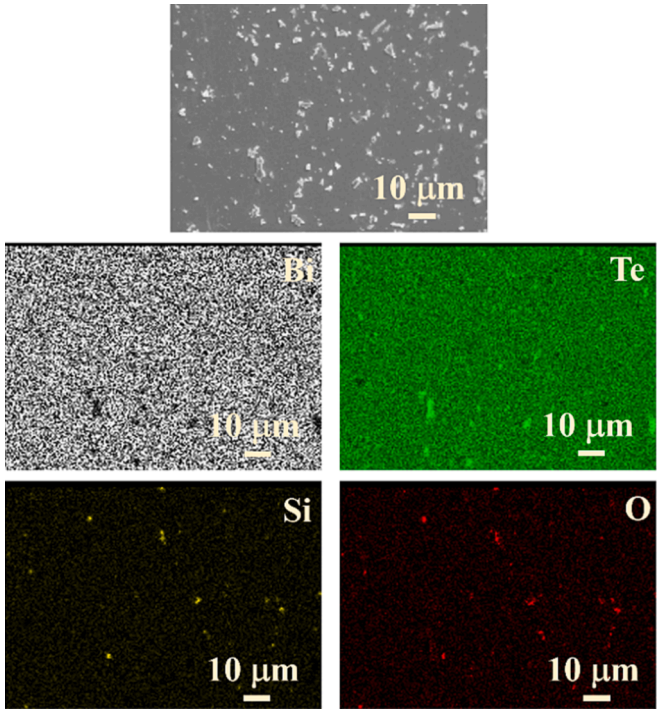


**Fig. 2.** Example of SEM image and EDS elements maps on $Bi_2Te_3$ crystal grown by procedure I + FZ. Silicon and oxygen are detected because of the eventual interaction of the quartz tube with the material.

stoichiometry of the grown parent compounds and of the crystals with Se and Sb substitutions, i.e. $Bi_2Se_{0.9}Te_{2.1}$ and $Bi_{1.85}Sb_{0.15}Se_3$.

### 3.2. X-ray diffraction analyses

EBSD measurements on crystals of $Bi_2Te_3$ from batches of Fig. 1a) and 1c) confirm that the nature of samples after the growth with the Procedure II is still polycrystalline. The measurements are performed mounting the samples on a special stub where reference directions, i.e. normal (ND), rolling (RD) and transverse (TD) are fixed: using crystallographic database, a orientation color key (on the panel b) of Fig. 4) associates each color with a crystallographic orientation. Thus, in Fig. 4 the SEM images with the corresponding orientation maps obtained analysing crystals from procedure II alone (C1 – upper panel of Fig. 4) and from procedure II + FZ (C3 - lower panel of Fig. 4) are shown to directly compare their crystallographic features and to highlight the improvement of the quality of the sample in size and crystallinity by melting the samples by the FZ technique. The surface of the sample C1 is

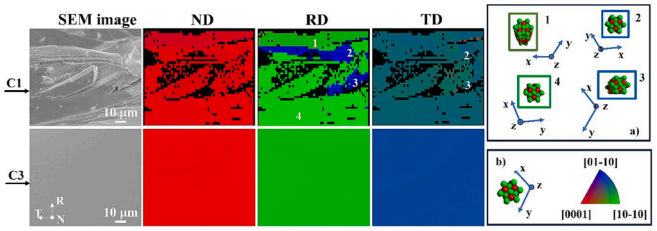


**Fig. 4.** Upper and lower panels show the SEM image and the three corresponding orientation maps of the crystal C1, grown by Procedure II alone, and of the crystal C3, grown by Procedure II + FZ, respectively. In panel a) are reported examples of crystalline cell representations of some crystals, denoted with 1, 2, 3 and 4, in the RD and TD maps of crystal C1. Panel b) shows the crystalline cell representation of the single crystal C3 and the orientation color key. For each cell, the axes orientation reference is reported.

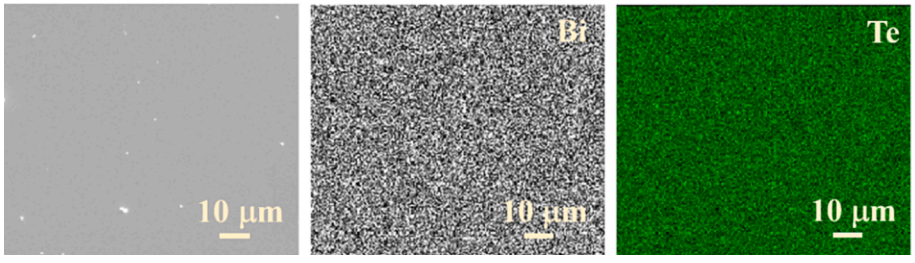


**Fig. 3.** Example of SEM image and EDS elements maps on $Bi_2Te_3$ crystals grown by procedure II + FZ. No impurities were detected in this case.

neither flat nor homogeneous reflecting the morphology of several crystals grown close to each other in different directions. In fact, the EBSD analysis points out that these crystals are on average oriented with the *c*-axis of the rhombohedral cell parallel to the ND (i.e. perpendicular to the growth direction), while their in plane orientations are randomly distributed. The RD and TD maps of crystal C1 do not have a single color: as an example, each shade of green (indicated as 1 and 4 points in the RD map) corresponds to a different crystalline cell orientation, as shown in panel a) of Fig. 4. Even the blue regions 2 and 3 correspond to slightly different cells, since in the TD map those areas have different color gradients. The second sample, C3, is a pure single crystal with the *c*-axis parallel to the ND and one of the in-plane crystallographic axis close to be parallel to the RD. For each direction, a single color is detected in the orientation maps which means that the crystalline cell has always the same orientation. It is worth noting that the uniform green colour in the RD map differs from the shades of green in the RD map of sample C1. Therefore, as shown in panel b) of Fig. 4, the crystalline cell of sample C3 is differently oriented from those of the areas 1 and 4 depicted in panel a) of Fig. 4, even though it is always around the [10–10] direction. The Fig. 5a) shows sample of $Bi_2Se_3$ taken out of the quartz tube from the set of FZ grown crystals after being through Procedure II. As an example, x-ray diffractograms acquired on crystals cleaved from this sample are reported in Fig. 5b). The red colored diffractogram belongs to the crystal indicated with (1) and shows only the (00 l) peaks of the trigonal space group R-3 m characteristic of the $Bi_2Se_3$.

In the black coloured diffractogram, that refers to the crystal indicated with (2), some impurity peaks were detected together with the (00 l) reflections of the desired phase. Since the crystal (2) was selected from a region of the boule in Fig. 5a) close to the surface touching the wall of the quartz tube, it is reasonable that the impurity peaks in the black coloured diffractogram may be due to some reaction of the material with the quartz. The impurity peaks could not be indexed to any known quartz phases or those in the Bi-Se phase diagram and we infer that any impurity phases present are in very small percentages.

Results similar to those obtained on the parent compound $Bi_2Te_3$ and $Bi_2Se_3$ are also observed on the compounds doped with Se and Sb, respectively. The Table 2 summarizes the sample characterization results. It is worth noticing that for each grown compound, it was possible to isolate large stoichiometric very well oriented single crystals with sizes ranging from few mm up to tens of mm, and varying thicknesses down to very thin flakes.

**Table 2**
Schematic account of the results obtained from the characterization of crystals of the Bi-Se-Sb and Bi-Se-Te systems grown following the Procedures described in the text.

| | Morphology | Composition | X-ray diffraction |
|---|---|---|---|
| **C1** | rough surface among small crystals | stoichiometric compounds | polycrystalline samples |
| **C2** | rough surface | traces of quartz in the crystals | not pure single crystals |
| **C3** | flat surface | stoichiometric compounds | pure single crystals |

* C1 means “crystals grown by Procedure II alone”, C2 means “crystals grown by Procedure I + FZ”, C3 means “crystals grown by Procedure II + FZ”.

The Fig. 6 shows the x-ray diffractograms of selected single crystals grown in the FZ. All the samples are (00 l) oriented with the peaks position corresponding to the crystalline structure characteristic of the Bi-chalcogenides. Each inset shows a picture of the measured sample, with nominal composition $Bi_2Te_3$ (Fig. 6a), $Bi_2Se_3$ (Fig. 6b), $Bi_2Se_{0.9}Te_{2.1}$ (Fig. 6c), and $Bi_{1.85}Sb_{0.15}Se_3$ (Fig. 6d). EDS analyses were carried out on several samples to confirm the stoichiometry of our compounds. On average, the following stoichiometric ratios were obtained for each compound: $Bi_{1.96}Te_{3.04}$, $Bi_{2.09}Se_{2.91}$, $Bi_{1.91}Se_{0.81}Te_{2.2}$, $Bi_{1.90}Sb_{0.15}Se_{2.95}$. The stoichiometric ratios were calculated from the EDS atomic percentages normalized to the total number of atoms in the compound. The analysis of the peak positions allowed to calculate the *c*-axis lattice parameter for each compounds as 30.534 (1) Å, 28.802 (3) Å, 29.735 (3) Å, 28.645 (1) Å, from panels of Fig. 6a, 6b, 6c and 6d, respectively. It is worth noting that the *c*-axis parameters of the $Bi_2Te_3$, $Bi_2Se_3$, and $Bi_2Se_{0.9}Te_{2.1}$ are in good agreement with the values reported in literature [6,8,21]. The *c*-axis lattice parameter obtained for the single crystal of the $Bi_{1.85}Sb_{0.15}Se_3$ is reported here, to the best of our knowledge, for the first time. Compared with the diffractograms of the $Bi_2Te_3$ and $Bi_2Se_3$ crystals, the reflections of rhombohedral structures of the doped compounds shift to larger angles (corresponding to lower *c*-xis lattice

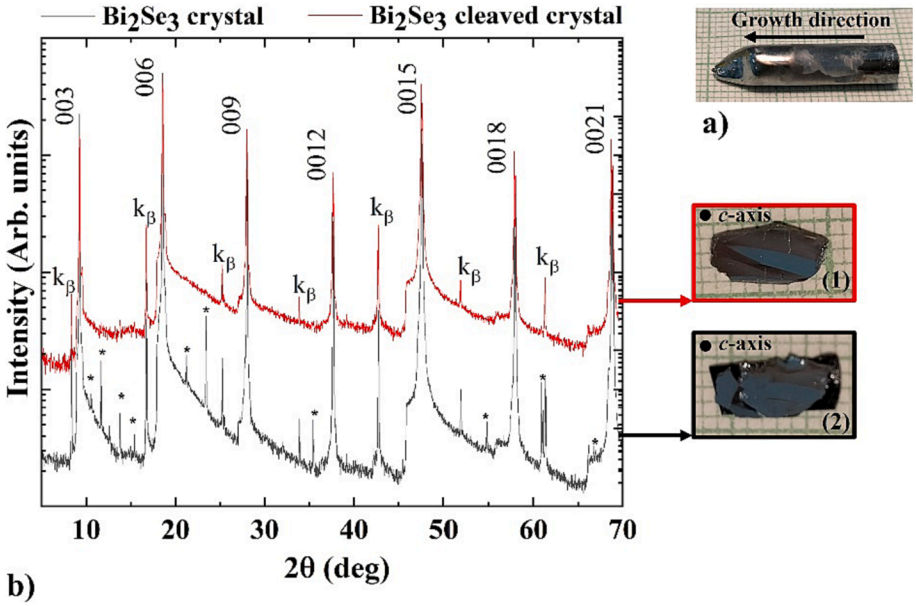


**Fig. 5.** a) Example of as grown $Bi_2Se_3$ boule from the set of FZ grown crystals following from Procedure II, with crystal growth direction parallel to the ab plane. b) X-ray diffractograms of the crystals indicated with (1) and (2) in the picture are red and black in the graph, respectively, as the corresponding outlines around the pictures. Cleaved crystals (1) and (2) from the boule in a) showing the direction of the c-axis. (For interpretation of the references to color in this figure legend, the reader is referred to the web version of this article.)

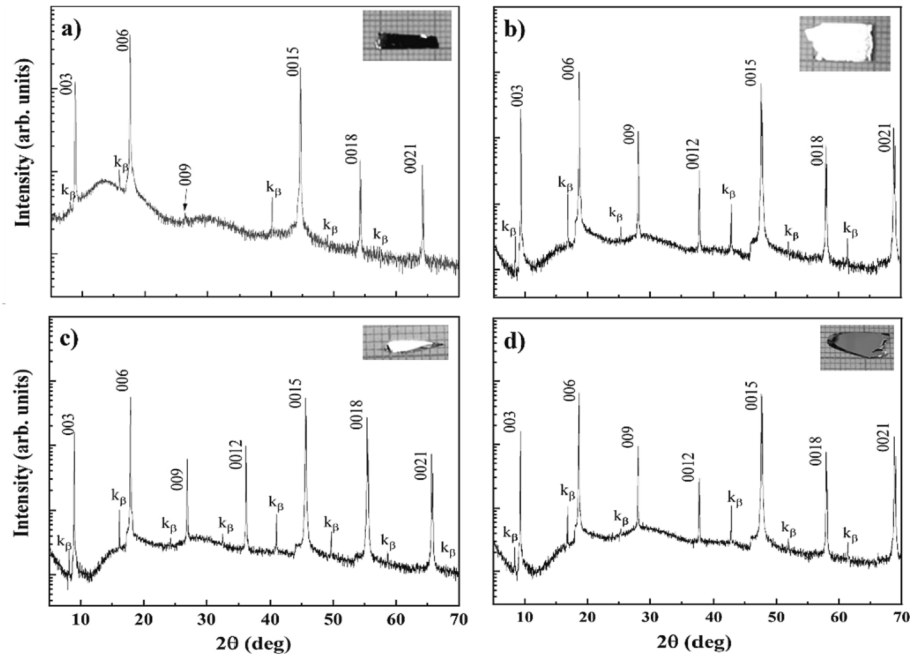


**Fig. 6.** X-ray diffractograms of selected single crystals grown in the FZ: a) $Bi_2Te_3$, b) $Bi_2Se_3$, c) $Bi_2Se_{0.9}Te_{2.1}$, d) $Bi_{1.85}Sb_{0.15}Se_3$. Each inset shows a picture of the measured sample.

parameters) consistently with the introduction in the structures of the Se and Sb atoms, with lower atomic radii (117 pm and 141 pm) compared to Te (143 pm) and Bi (155 pm), respectively. The crystals' quality was estimated by measuring the full width at half maximum (FWHM) around the (0015) reflections of each compound, ranging between 0.014° and 0.068°.

## 4. Conclusion

Two procedures for growing Bi-based chalcogenide single crystals were optimized to obtain high quality stoichiometric compounds by using optical floating zone technique. A series of samples with four different stoichiometries were successfully grown, i.e. $Bi_2Te_3$, $Bi_2Se_3$, $Bi_2Se_{0.9}Te_{2.1}$, $Bi_{1.85}Sb_{0.15}Se_3$, with the crystal sizes obtained ranging from a few mm up to tens of millimeters, and from bulk thicknessess to very thin flakes. The morphological and compositional analyses have enabled us to identify the best growth procedure, i.e the procedure II + FZ, to obtain large crystals with flat surfaces, uniform and homogeneous elemental distribution, without presence of impurities. EBSD investigations provided details of the crystalline local structure of the samples, giving further evidence about the best quality of the samples grown by Procedure II + FZ. X-ray diffraction analysis confirmed the formation of rhombohedral crystal structure in R-3 m phase for all the studied compounds, and the good agreement of the *c*-axis lattice parameters values with respect to the data in the literature. In particular, the value obtained for the single crystal of the $Bi_{1.85}Sb_{0.15}Se_3$ is reported here, to the best of our knowledge, for the first time. The high quality of the crystals was confirmed by evaluating the FWHM of the most intense peaks in the diffractogram of each compound obtaining values in the range between 0.014° and 0.068°.

## Declaration of competing interest

The authors declare that they have no known competing financial interests or personal relationships that could have appeared to influence the work reported in this paper.

## Data availability

The data that supports the findings of this study are available in the paper itself.

## Acknowledgements

This work was financially supported by PRIN 2020 project Conquest funded by the Italian Ministry of University and Research (Prot. 2020JZ5N9M). The authors wish to thank the CNR for funding the visit of Prof. Balakrishnan in the framework of the Short Term Mobility Program – 2022. G.B. also wishes to thank EPSRC, United Kingdom for funding through EP/T005963/1. The authors thank Jae-Hyuck Lee for helpful discussions.

## References

[1] G.S. Hegde, A.N.A. Prabhu, Review on doped/composite bismuth chalcogenide compounds for thermoelectric device applications: various synthesis techniques and challenges, J. Electr. Mat. 51 (2022) 2014.
[2] K. Mazumde, P.M. Shirage, A brief review of $Bi_2Se_3$ based topological insulator: From fundamentals to applications, J. Alloys Comp. 888 (2021) 161492.
[3] M.M. Sharma, P. Sharma, N.K. Karn, V.P.S. Awana, Comprehensive review on topological superconducting materials and interfaces, Supercond. Sci. Technol. 35 (2022) 083003.
[4] N. Kumar, S.N. Guin, K. Manna, C. Shekhar Claudia Felser, Topological quantum materials from the viewpoint of chemistry, Chem. Rev. 121 (2021) 2780.
[5] V.V. Atuchin, V.A. Golyashov, K.A. Kokh, I.V. Korolkov, A.S. Kozhukhov, V. N. Kruchinin, S.V. Makarenko, L.D. Pokrovsky, I.P. Prosvirin, K.N. Romanyuk, O. E. Tereshchenko, Formation of Inert $Bi_2Se_3$(0001) cleaved surface, Cryst. Growth Des. 11 (2011) 5507.
[6] V.V. Atuchin, V.A. Golyashov, K.A. Kokh, I.V. Korolkov, A.S. Kozhukhov, V. N. Kruchinin, I.D. Loshkarev, L.D. Pokrovsky, I.P. Prosvirin, K.N. Romanyuk, O. E. Tereshchenko, Crystal growth of $Bi_2Te_3$ and noble cleaved (0001) surface properties, J. Solid State Chem. 236 (2016) 203.
[7] R.A. Laudise, W.A. Sunder, R.L. Barns, R.J. Cava, T.Y. Kometani, Czochralski growth of doped single crystals of $Bi_2Te_3$, J. Cryst. Growth 94 (1989) 53.
[8] G. Awana, R. Sultana, P.K. Maheshwari, R. Goyal, B. Gahtori, A. Gupta, V.P. S. Awana, Growth and magneto-transport of $Bi_2Se_3$ single crystals, J. Supercond. Nov. Magn. 30 (2017) 853.
[9] P. Chen, D. Zhou, P. Li, Y. Cui, Y. Chen, The preparation process and feature of the topological insulator $Bi_2Te_3$, J. Mod. Transport. 22 (2014) 59.
[10] J. Yuan, M. Zhao, W. Yu, Y. Lu, C. Chen, M. Xu, S. Li, K.P. Loh, B. Qiaoliang, Spectroscopy of two-dimensional $Bi_2Te_xSe_{3-x}$ platelets produced by solvothermal method, Materials 8 (2015) 5007.

[11] S. Gautam, B. Singh, V. Aggarwal, M.S. Kumar, V.N. Singh, C.P. Singh, S. S. Kushvaha, Thickness dependent optical properties of sputtered $Bi_2Se_3$ films on mica, Mater. Today:. Proc. 64 (2022) 1725.
[12] M. Salvato, M. Scagliotti, M. De Crescenzi, P. Castrucci, F. De Matteis, M. Crivellari, S. Pelli Cresi, D. Catone, T. Bauch, F. Lombardi, Stoichiometric $Bi_2Se_3$ topological insulator ultra-thin films obtained through a new fabrication process for optoelectronic applications, Nanoscale 12 (2020) 12405.
[13] S.-M. Huang, S.-Yu Lin, J.-F. Chen, C.-K. Lee, S.-H. Yu, M.M.C. Chou, C.-M. Cheng, H.-D. Yang, Shubnikov–de Haas oscillation of $Bi_2Te_3$ topological insulators with cm-scale uniformity, J. Phys. D: Appl. Phys. 49 (2016) 255303.
[14] A. Akrap, M. Tran, A. Ubaldini, J. Teyssier, E. Giannini, D. van der Marel, P. Lerch, C.C. Home, Optical properties of $Bi_2Te_2Se$ at ambient and high pressures, Phys. Rev. B 86 (2012) 235207.
[15] Y. Tian, S. Jia, R.J. Cava, R. Zhong, J. Schneeloch, G. Gu, K.S. Burch, Understanding the evolution of anomalous anharmonicity in $Bi_2Te_{3-x}Se_x$, Phys. Rev. B 95 (2017) 094104.
[16] M.D. Anoop, J. Yadav, N. Yadav, R. Singh, K. Shinzato, S.N. Dolia, A. Jain, T. Ichikawa, M. Kumar, Effect of isovalent substitution on the structural and electrical properties of $Bi_xSb_{2-x}Te_3$ topological insulator single crystals, Mater. Today:. Proc. 31 (2020) 616.
[17] A. Akrap, A. Ubaldini, E. Giannini, L. Forró, $Bi_2Te_{3-x}Se_x$ series studied by resistivity and thermopower, Europhys. Lett. 107 (2014) 57008.
[18] P. Shyni, P.P. Pradyumnan, Fermi level tuning in modified Bi2Te3 system for thermoelectric applications, Royal Soc. Chem. Adv. 11 (2021) 4539.
[19] I. Şişman, M. Biçer, Structural, morphological and optical properties of $Bi_{2-x}Sb_xSe_3$ thin films grown by electrodeposition, J. Alloys Compd. 509 (2011) 1538.
[20] P.-H. Lin, S.-W. Chen, J.-D. Hwang, H.-S. Chu, Liquidus projections of Bi-Se-Ga and Bi-Se-Te ternary systems, Metallurg. Mater. Trans. E 3 (4) (2016) 281–290.
[21] G.N. Kozhemyakin, Y.S. Belov, A.N. Parashenko, V.V. Artemov, O.N. Soklakova, Morphology and nanostructured features in BiSbTe and BiSeTe solid solutions obtained by hot extrusion, Mater. Sci. Eng. B 271 (2021) 115270.